Publication I

Jari Holopainen, Risto Valkonen, Outi Kivekäs, Janne Ilvonen, and Pertti Vainikainen. 2010. Broadband equivalent circuit model for capacitive coupling element–based mobile terminal antenna. IEEE Antennas and Wireless Propagation Letters, volume 9, pages 716-719.

Broadband Equivalent Circuit Model for Capacitive Coupling Element–Based Mobile Terminal Antenna

Jari Holopainen, Risto Valkonen, Outi Kivekäs, Janne Ilvonen, and Pertti Vainikainen

***Abstract*—In this letter, it is shown how the behavior of a capacitive coupling element (CCE)-based mobile terminal antenna can be modeled at the UHF band as a combination of the separate wave-modes of the structure. The proposed equivalent circuit model improves the general understanding of the operation of the antenna structure. It can be used for analyzing the combined performance of the capacitive coupling element and terminal chassis, but it also helps in analyzing how different parts of the antenna structure contribute to the impedance and radiation.**

***Index Terms*—Antenna theory, capacitive coupling elements (CCE), equivalent circuits, microstrip antennas, mobile antennas.**

I. INTRODUCTION

CAPACITIVE coupling elements (CCE) are an antenna concept applied to UHF-band digital television or cellular system antennas in mobile terminals; see, e.g., [1]–[5]. The CCE has many benefits based on its fundamental property of exploiting the radiation of the metallic chassis of the mobile terminal. The element is just designed to optimize the coupling between the transceiver and free-space electromagnetic (EM) waves at a wide frequency range. Consequently, the antenna does not have to be made self-resonant since it is matched with an external matching circuitry at any desired frequency band. Since the CCE is not self-resonant, it can be made more compact than, e.g., a planar inverted-F antenna (PIFA) at frequencies below 1 GHz. In addition, the CCE is not frequency-selective, which enables easy frequency reconfigurability. Also, the design of a CCE antenna is relatively simple, as the matching is created outside the CCE.

This work aims at an improved overall understanding of the operation of CCE antennas. To realize this, an equivalent circuit model for a typical CCE antenna is developed. The circuit is based on coupled resonators, which model the wavemodes of the antenna. Thus, the work in [6] provides a general basis for the more advanced model proposed in this letter. All the significant wavemodes of the CCE antenna are modeled at the UHF band (0.3–3 GHz), which makes the proposed model fairly broadband. The circuit model provides a useful circuit-theoretical tool for analyzing the combined performance of the antenna element and the terminal chassis, but it also helps in analyzing
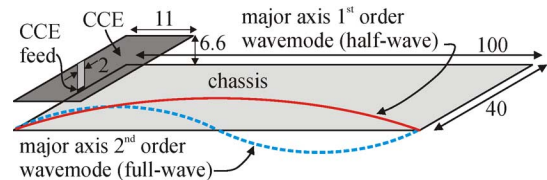
Fig. 1. Typical capacitive coupling element (CCE) mounted on a thin mobile terminal chassis, with principal current distributions of the two lowest order major axis wavemodes of the chassis. Dimensions are in millimeters.

how different parts of the structure contribute to the radiation and input impedance of the entire structure.

II. CAPACITIVE COUPLING ELEMENT ANTENNA WAVEMODES

Fig. 1 shows a simple CCE antenna geometry. Below 2 GHz, the mobile terminal chassis (size 100×40 mm^2) is the main radiator of the structure, and especially below 1 GHz the role of the CCE is just to efficiently couple radiant currents to the low-Q wavemode of the chassis [1], [6]. At higher UHF frequencies, the radiation of the CCE becomes also significant. The antenna can be matched at any selected frequency because the resonance is produced with a suitable matching circuitry placed next to the CCE feed [1]. The circuit model in this letter is derived for the particular structure shown in Fig. 1 only, but the same derivation procedure could be applied to other CCE structures with changed shape or dimensions.

A. Mobile Terminal Chassis

As is well known, the terminal chassis supports flat dipole-type current distributions and has certain resonant wavemodes [6], [7]. The characteristic mode theory provides a useful tool to study the radiation characteristics of the wavemodes of the plain chassis. It is possible to numerically calculate the resonant frequencies and the respective quality factors. In [8], the method was applied to analyze the typical-sized, 100×40 mm^2, thin mobile terminal chassis. The first four resonant frequencies of the wavemodes are 1.26, 2.68, 2.74, and 3.08 GHz, and the respective Q values are 2.3, 3.0, 2.5, and 2.3. The first two modes represent the major axis half- and full-wave dipole modes; see Fig. 1. The third mode at 2.74 GHz is the minor axis half-wave mode, and the fourth mode at 3.08 GHz is the magnetic dipole mode. In practice, the current distribution of the chassis at a given frequency is the superposition of these wavemodes. The third major axis wavemode is above 4 GHz and thus outside the UHF band.

The characteristic mode analysis is based on applying a plane wave excitation on the chassis. However, in CCE antennas, it is the CCE that excites the chassis wavemodes. Thus, the CCE significantly affects the excitation of the wavemodes and also
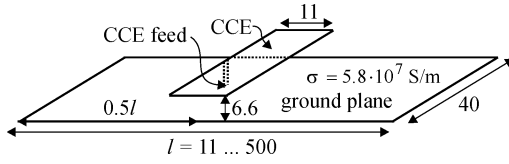
Fig. 2. CCE mounted in the midpoint of a variable-length ground plane. Dimensions are in millimeters. The CCE itself is identical to that shown in Fig. 1.

Fig. 3. Circuit blocks of the equivalent circuit model.

slightly tunes downward the respective resonant frequencies [9]. Furthermore, it is the location of the CCE feed that mainly determines which modes are excited. Placing the feed in the midpoint of the short edge of the chassis, as in Fig. 1, results in efficient excitation of only the major axis modes of the chassis. For example, a feed placed in the corner of the chassis could excite all four mentioned wavemodes.

B. Capacitive Coupling Element

The operation of the CCE can be studied with the help of EM simulations by placing the element in the midpoint of a variable-length ground plane; see Fig. 2. The ground plane length at which the unloaded quality factor has a maximum can be assumed to present a case, where the effect of the ground plane wavemodes is smallest and in that case the quality factor is determined mainly by the CCE alone. This method can be used since the impedance and radiation properties of the CCE are determined by its current distribution, which does not change considerably when the element is located in the open end of a terminal chassis as in Fig. 1 [6], [10]. The operation of the structure is analyzed with a method-of-moments–based electromagnetic simulator IE3D (ver. 14.5) by Zeland. The Q value is calculated from the simulated impedance using the equation valid for small antennas introduced in [11].

The maximum of the unloaded quality factor was found in the case when the length of the ground plane was 31 mm. The simulation results propose that the impedance behavior of the CCE at UHF frequencies is similar to that of a top-loaded monopole on a ground plane [12]. Thus, this operation mode of CCE is called the *monopole mode*. The fundamental frequency of the monopole mode—i.e., the frequency at which the reactance is zero—is $f_{\mathrm{r,mm}} = 1.78$ GHz. The radiation resistance is directly proportional to the square of the frequency. Thus, the resistance behavior R_{mm} of the monopole mode can be modeled with good accuracy as a function of frequency f

$$R_{\mathrm{mm}}(f) = R_0 \left(\frac{f}{f_{\mathrm{r,mm}}}\right)^2 \qquad (1)$$

where $R_0 = 1.46\ \Omega$ is the input resistance at $f_{\mathrm{r,mm}}$. $Q_{\mathrm{mm}} = 41$ at 1.78 GHz. The location of the feed somewhat affects the fundamental frequency and the respective resistance. A feed point displaced from the midpoint of the long axis of the CCE would cause a decrease in the fundamental frequency as well as in the respective resistance. However, in this letter we concentrate only on the midpoint-placed feed as in Fig. 1.

Other wavemodes can also be recognized. The CCE can operate like a traditional microstrip patch antenna at suitable frequencies. The resonant frequency of the lowest order half-wave
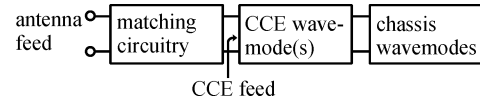
"patch antenna wavemode" can be obtained from the basic design formulas (or, e.g., EM simulations), and it is about 3.3 GHz. It is well known that the excitation of the wavemode largely depends on the location of the CCE feed. If the feed was placed in the midpoint of the long edge of the CCE, as in Fig. 2, the excitation of the half-wave mode would be weak because there is an electric field zero in the midpoint of the long axis of the CCE. The second-order full-wave mode occurs at about 7 GHz, and thus it is assumed not to significantly affect the CCE operation at the UHF band (0.3–3 GHz).

III. EQUIVALENT CIRCUIT MODEL

A highly accurate broadband model of the input impedance of a CCE antenna could be derived using standard circuit synthesis methods, but this approach would lose physical information on the contribution of each part of the structure on the radiation and impedance. Instead, a simple model based on the excited wavemodes will give a better physical explanation of the operation of the CCE antenna.

The currents flowing on the surface of the chassis are induced through the electromagnetic coupling from the CCE, which is further excited by the CCE feed (see Fig. 1) through the matching circuitry from the antenna feed. Thus, the antenna structure is modeled as a chain of circuit blocks that represent the chassis, CCE, and matching circuitry; see Fig. 3. Each of the excited wavemodes of the CCE and the chassis are modeled using an *RLC* resonator circuit, and the combination of the wavemodes as a set of coupled resonators. Furthermore, the component values of the *RLC* resonators are determined from the reported resonant frequencies and the respective unloaded quality factors; see Section II. The coupling between the resonators is modeled as an ideal transformer, an approach adopted from [6]. An alternative way to model the coupling between the wavemodes is to use, e.g., an impedance inverter [7].

A. CCE Resonator Model

First, a circuit model for the CCE block is derived without the effect of the chassis wavemodes. As discussed, the excitation of the CCE half-wave mode is weak with the midpoint feed, and the full-wave mode at about 7 GHz has no significance at the UHF band. Therefore, we need to model only the monopole mode. The CCE circuit topology is shown in Fig. 4. The used *RLC* circuit is series-type, which is customary for a monopole-type antenna, as proposed also in [7]. The parallel capacitor C_{p} in Fig. 4 is a parasitic component, which is required to satisfy the condition of zero impedance at infinite frequency for the CCE feed. Its physical interpretation is the capacitance between the CCE feeding pin and the ground plane.

In the case of a displaced feed, the half-wave mode could as well be modeled with another series-type *RLC* resonator placed
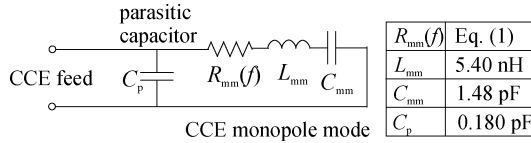
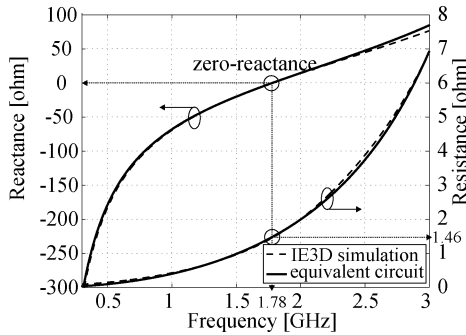Fig. 4. Circuit topology and the defined component values for the CCE without the effect of the chassis.

Fig. 5. Impedances seen from the CCE feed of the circuit model and the IE3D simulated CCE structure shown in Fig. 2.
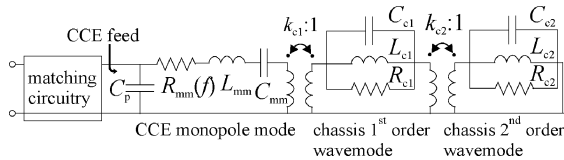

Fig. 6. Circuit topology for the CCE antenna with the effect of the chassis two lowest order wavemodes.

parallel to the monopole mode resonator. The effect of the location of the feed on the coupling to the half-wave mode can be modeled with an ideal transformer.

The resistance R_{mm} of the monopole mode is given in (1). The component values L_{mm} and C_{mm} are chosen unambiguously so that they implement the fundamental frequency $f_{\mathrm{r,mm}} = 1.78$ GHz and $Q_{\mathrm{mm}} = 41$ at $f_{\mathrm{r,mm}}$ (see Section II-B). The value of the parasitic capacitor C_{p} is difficult to estimate. It is here defined based on the comparison between the impedances of the circuit and the IE3D simulation. The impedances seen from the CCE feed of the circuit model and the respective IE3D simulation are shown in Fig. 5. It can be seen that very good agreement can be achieved.

B. CCE Antenna With Effect of Terminal Chassis

Next, the effect of the terminal chassis as in Fig. 1 is taken into account. The proposed circuit topology is shown in Fig. 6. As the CCE resonator was chosen to be series-type, the chassis resonators need to be parallel-type in order to avoid the use of impedance inverters in the equivalent circuit [13]. In addition, these two parallel-type resonators modeling the excited chassis wavemodes need to be in series. The electromagnetic coupling between the CCE and chassis wavemodes is modeled with an ideal transformer, which gives the impedance scaling (factor k_{c1}) between the resonators [6]. Another transformer (with scaling factor k_{c2}) is required since the coupling from the
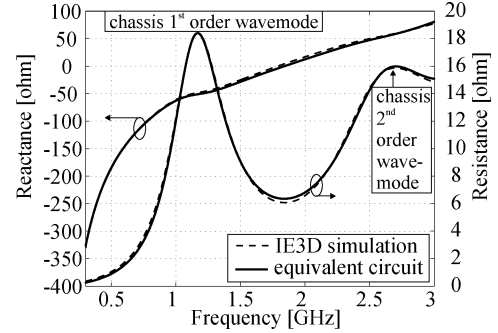

Fig. 7. Comparison between the impedances seen from the CCE feed of the circuit model and the IE3D simulated CCE structure shown in Fig. 1.

TABLE I
COMPONENT VALUES OF THE EQUIVALENT CIRCUIT IN FIG. 6.

wavemode	L [nH]	C [pF]	R [Ω]	f_{r} [GHz]	Q_{rad}	other components
monopole	5.80	1.39	1.46	1.77	44	$C_{\mathrm{p}} = 0.18$ pF
chassis 1st	1.18	15.8	20.3	1.17	2.3	$k_{\mathrm{c1}} = 1.0$
chassis 2nd	0.151	24.7	7.39	2.61	3.0	$k_{\mathrm{c2}} = 1.0$

CCE wavemode to the second-order wavemode of the chassis might not be the same as to the first-order mode.

The initial component values of the chassis resonators are derived using the reported (see Section II-A) resonant frequencies and respective Q values of the chassis wavemodes, with the help of the IE3D simulated input impedance of the entire CCE antenna structure, which gives the resistance values for the resonators. The impedance scaling factors are free parameters, and their values are chosen to be $k_{\mathrm{c1}} = k_{\mathrm{c2}} = 1$. Thus, in theory, the transformers could be left out, but since they have important physical significance, they are not removed from the circuit model. For example, if the location of the CCE relative to the chassis was changed, the coupling from the CCE to the chassis wavemodes would vary, and thus this effect could be modeled by varying the scaling factors k_{c1} and k_{c2}.

As stated in [9], the resonant frequencies of the chassis wavemodes are slightly tuned downward from the ones reported in Section II-A due to the CCE excitation. Thus, in order to have a good agreement with the IE3D-simulated impedance, the component values of the resonators need to be slightly fine-tuned from the initial values. The final values, resonant frequencies, and unloaded quality factors are shown in Table I. The impedances seen from the CCE feed of the circuit model and the respective IE3D simulation are shown in Fig. 7. It can be seen that the principal impedance behavior of the CCE antenna can be modeled with the proposed circuit model. In fact, a very good agreement with the IE3D simulation can also be achieved since the maximum absolute errors of the resistance and reactance are only 0.30 Ω (at 0.74 GHz) and 4.2 Ω (at 1.8 GHz), respectively.

IV. EFFECT OF CHASSIS WAVEMODES ON IMPEDANCE, BANDWIDTH POTENTIAL, AND RADIATION

The proposed circuit model can be used to separate the effect of the chassis wavemodes on the impedance, bandwidth potential (concept introduced, e.g., in [14]), and radiation. The impedance and bandwidth potential calculated from the circuit
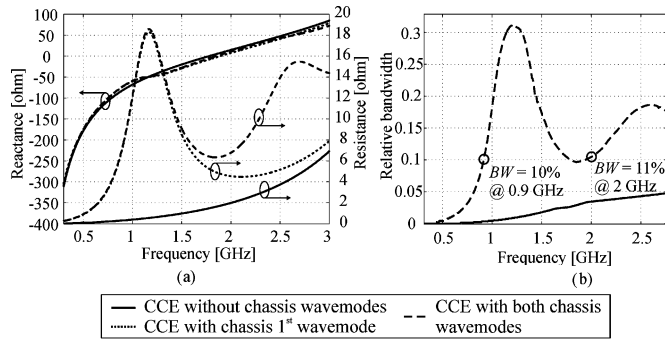
Fig. 8. Effect of the chassis wavemodes on the (a) impedance and (b) 6-db return-loss bandwidth potential, with calculations performed by the circuit model.
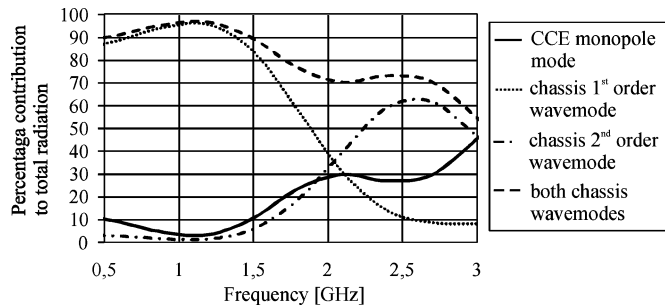

Fig. 9. Percentage contribution of each wavemode to the total radiation losses of the circuit model.

model with and without the effect of the chassis wavemodes are shown in Fig. 8. First, in Fig. 8(a), the reactance behavior is mainly determined by the CCE monopole mode. This is due to the fact that the Q value of the CCE is much higher than that of the chassis wavemodes. Only minor changes in the reactance can be seen due to the chassis wavemodes. On the other hand, the resistance behavior is mainly determined by the chassis wavemodes. That is due to the fact that the CCE effectively excites the chassis wavemodes at a wide frequency band. Especially at the lower UHF frequencies, the effect of the chassis wavemode on the resistance is dominant since the effective resistance of the CCE is extremely small. The same observation can also be made from the bandwidth potential curves in Fig. 8(b). It can be concluded that the operation of the current cellular systems, especially at the 0.9-GHz range, would not be possible without the contribution of the chassis.

Finally, the contribution of each resonator to the radiation is analyzed. For an antenna with fully high-conductivity metal structure, as in Fig. 1, the radiation efficiency is very close to 1 at the UHF frequencies. Thus, it can be expected that all the losses are caused by radiation. The percentage contribution of each wavemode to the total radiation "losses," calculated by the equivalent circuit, is shown in Fig. 9. It can be seen that the contribution of the chassis wavemodes to the radiation is very significant. At the 1-GHz frequency range, as much as 95% is radiated by the chassis wavemodes. This is fully supported by the results calculated from the surface integrals of the EM-simulated chassis current distributions in [1]. Furthermore, at the 2-GHz range, the chassis still contributes at least 70%, which is also consistent with the results in [1].

V. Conclusion

In this letter, a broadband equivalent circuit model is proposed for a typical example of a capacitive coupling element (CCE) antenna structure. A very good agreement of the input impedance behavior between EM simulation and the wave-mode-modeling-based equivalent circuit was achieved. The circuit model is a useful tool for improving the general understanding of the CCE antennas, as well as for analyzing the effect of each part of the antenna structure on the impedance, bandwidth, and radiation. The usable frequency band of the circuit model could be extended by introducing more wavemodes into the circuit. A similar model derivation method could also be applied to other wideband coupling-based antenna structures, such as the inductive coupling element or direct feed. The next step is to model the effect of lossy dielectric material on each wavemode and, based on that, study the effect of the user with the help of the equivalent circuit. This could improve general understanding of the effect of the user on mobile terminal antennas and eventually decrease also the computational complexity of user effect estimation.

References

[1] J. Villanen, J. Ollikainen, O. Kivekäs, and P. Vainikainen, "Coupling element based mobile terminal antenna structures," *IEEE Trans. Antennas Propag.*, vol. 54, no. 7, pp. 2142–2153, Jul. 2006.

[2] J. Holopainen, O. Kivekäs, C. Icheln, and P. Vainikainen, "Internal broadband antennas for digital television receiver in mobile terminals," *IEEE Trans. Antennas Propag.*, 2010, to be published.

[3] R. Valkonen, C. Luxey, J. Holopainen, C. Icheln, and P. Vainikainen, "Frequency-reconfigurable mobile terminal antenna with MEMS switches," in *Proc. 4th EuCAP*, Barcelona, Spain, Apr. 12–16, 2010, pp. 1–5.

[4] D. Manteuffel and M. Arnold, "Considerations for reconfigurable multi-standard antennas for mobile terminals," in *Proc. IEEE iWAT, Small Antennas Novel Metamater.*, Chiba, Japan, Mar. 4–6, 2008, pp. 231–234.

[5] Z. H. Hu, C. T. P. Song, J. Kelly, P. S. Hall, and P. Gardner, "Wide tunable dual-band reconfigurable antenna," *Electron. Lett.*, vol. 45, no. 22, pp. 1109–1110, Oct. 2009.

[6] P. Vainikainen, J. Ollikainen, O. Kivekäs, and I. Kelander, "Resonator-based analysis of the combination of mobile handset antenna and chassis," *IEEE Trans. Antennas Propag.*, vol. 50, no. 10, pp. 1433–1444, Oct. 2002.

[7] U. Bulus and K. Sohlbach, "Modelling of the monopole interaction with a small chassis," in *Proc. 3rd EuCAP*, Berlin, Germany, Mar. 23–27, 2009.

[8] C. T. Famdie, W. L. Schroeder, and K. Solbach, "Numerical analysis of characteristic modes on the chassis of mobile phones," in *EuCAP 2006 1st European Conf. Antennas Propag.*, Nice, France, Nov. 6–10, 2006, pp. 358–361.

[9] J. Rahola and J. Ollikainen, "Optimal antenna placement for mobile terminals using characteristic wavemodes," in *Proc. 1st EuCAP*, Nice, France, Nov. 6–10, 2006, pp. 1–6.

[10] T. Taga, "Analysis of planar inverted-F antennas and antenna design for portable radio equipment," in *Analysis, Design and Measurement of Small and Low-Profile Antennas*, K. Hirasawa and M. Haneishi, Eds. Norwood, MA: Artech House, 1992, ch. 5, pp. 161–180.

[11] A. D. Yaghjian and S. R. Best, "Impedance, bandwidth, and Q of antennas," *IEEE Trans. Antennas Propag.*, vol. 53, no. 4, pp. 1298–1324, Apr. 2005.

[12] K. Fujimoto, A. Henderson, A. Hirasawa, and J. R. James, *Small Antennas.* New York: Wiley, 1988.

[13] G. L. Matthaei, L. Young, and E. M. T. Jones, *Microwave Filters, Impedance Matching Networks and Coupling Structures.* New York: McGraw-Hill, 1964.

[14] J. Rahola, "Bandwidth potential and electromagnetic isolation: Tools for analysing the impedance behaviour of antenna systems," in *Proc. 3rd EuCAP*, Berlin, Germany, Mar. 23–27, 2009, pp. 944–948.